Adsorption of Semiflexible Polymers

Catharina C. van der Linden,* Frans A. M. Leermakers, and G. J. Fleer

Department of Physical and Colloid Chemistry, Dreijenplein 6,
6703 HB Wageningen, The Netherlands

Received March 24, 1995; Revised Manuscript Received September 25, 1995[⊗]

ABSTRACT: The self-consistent-field model for polymer adsorption of Scheutjens and Fleer is extended to the case of semiflexible chains in a cubic lattice. It is found that the scaling behavior for adsorption from a dilute solution of polymers with the same radius of gyration, but with a varying degree of stiffness, is markedly different. Adsorption from a semidilute solution gives a chain-length-independent profile, even when bond correlations are taken into account. Adsorbing block copolymers with blocks that differ only in the rigidity of the blocks adsorb with the stiffer block on the surface. This preference has an entropical origin. Such copolymers behave similar to "energetic" block copolymers, where the blocks differ in energetic interaction with the solvent or with the surface. The effects of chain stiffness are of the same order of magnitude as energetic effects.

Introduction

The first theoretical model for polymers was probably the random-walk model by Kuhn.[1] In this model, a polymer molecule is taken to consist of randomly jointed segments; *i.e.*, the orientation of each segment is independent of all the others. In practice, the backbone of a polymer molecule is not completely flexible: the segments cannot fold back onto themselves, and usually bond angles are restricted to specific values determined by the hybridization of the constituent atoms. However, this is not necessarily a problem; the chain-length dependence of the radius of gyration of an ideal polymer chain does not change if the bond angles are restricted, provided a number of bonds are combined into one statistical unit, which in turn can rotate independently. Still, it can be necessary to model chain stiffness; the fact that the radius of gyration can be rescaled properly does not imply that other parameters in more complicated systems are not altered. Also, if the polymer is very stiff, the statistical units become so large that for a finite chain length there are too few units to get reliable statistics. This is the "wormlike chain" case,[2,3] in which the persistence length of the chain plays a key role. The persistence length is a measure for the distance over which the polymer chain is stiff. By comparing the adsorption characteristics for polymers differing in flexibility but having the same radius of gyration it is possible to check whether rescaling works also in the case of adsorption.

Most of the research about semiflexible polymers is devoted to isotropic−nematic transitions, which is important for the field of polymer liquid crystals. An excellent review on these systems was written by Odijk;[4] we will not discuss them here.

Yethiraj *et al.*[5] recently found that in a polymer blend containing stiff and flexible molecules the stiff molecules segregate to the surface. This is a purely entropic effect: the stiffer polymers lose less entropy when adsorbing than the flexible ones. The theory to be presented below allows for molecules that have rigid and flexible blocks. In a sense, these molecules can be considered to be block copolymers, although the blocks do not differ in mixing or adsorption energy. Thus, we can investigate the entropic effects of surface segregation of block copolymers. Usually in block copolymer systems one does not include the effect of the difference in local chain rigidity, although it is often present. One of the goals of this paper is to investigate the problems encountered in this approach.

Theory

The model is based on the self-consistent-field theory for homopolymer adsorption by Scheutjens and Fleer,[6] using extensions for copolymers,[7] chain stiffness in a cubic lattice,[8] and bond correlations.[9] We use a simple cubic lattice. A polymer molecule consists of N segments, where the diameter of a segment equals the lattice spacing. Layers are chosen parallel to the (flat) surface and numbered $z = 0$ (the surface), 1 (the layer immediately adjoining the surface), to M (in the bulk solution, far from the surface). The volume fraction of segment number s of molecule i in layer z is $\varphi_i(z,s)$. If molecule i consists of more than one monomer type, we can define $\varphi_{Ai}(z)$ as the contribution of segment type A to the volume fraction of component i in layer z.

Interactions. The relative preference of a free monomer of type A to be in layer z with respect to the bulk solution is denoted as $G_A(z)$, the free segment distribution function. It can be related to the potential energy $u_A(z)$ of monomer type A in layer z using a Boltzmann equation:

$$G_A(z) = \exp(-u_A(z)/kT) \qquad (1)$$

In this equation, T is the absolute temperature and k Boltzmann's constant. The potential energy consists of two contributions: hard-core and energetic interactions: $u_A(z) = u'(z) + u_A^{int}(z)$. The hard-core contribution $u'(z)$ is calculated numerically by demanding that the lattice is completely filled with solvent molecules and polymer segments, *i.e.*, $\sum_{i,s}\varphi_i(z,s) = 1$ for any z. For the energetic interactions, we use a Bragg−Williams or random-mixing approximation:

$$u_A^{int}(z) = \sum_B \chi_{AB}(\langle\varphi_B(z)\rangle - \varphi_B^b) \qquad (2)$$

where φ_B^b stands for the volume fraction of monomer type B in the bulk, χ_{AB} is the Flory−Huggins interaction parameter between A and B, and $\langle\varphi_B(z)\rangle$ is the so-called neighbor-average of B around layer z:

$$\langle\varphi_B(z)\rangle = \sum_{d=-1,0,1} \lambda_d \varphi_B(z + d) \qquad (3)$$

where d is one of the three directions in the lattice: from

[⊗] Abstract published in *Advance ACS Abstracts,* January 15, 1996.

0024-9297/96/2229-1172$12.00/0 © 1996 American Chemical Society

layer z to layer $z - 1$ ("down") $d = -1$, within layer z ("sidewards") $d = 0$, or from layer z to layer $z + 1$ ("up") $d = 1$. For a simple cubic lattice $\lambda_{-1} = \lambda_1 = {}^1/_6$ and $\lambda_0 = {}^4/_6$.

The adsorption energy is included in eq 2 by taking the surface S as a separate component, with volume fraction $\varphi_S(z) = 1$ for $z < 1$ and $\varphi_S(z) = 0$ for $z \geq 1$. The resulting χ_{AS} relates to the more common Silberberg adsorption energy parameter χ_s[10] as $\chi_{AS} = -\lambda_{-1}\chi_s$, where all adsorption energies are calculated with respect to the solvent o, *i.e.*, $\chi_{oS} = 0$.

Bond Correlations. In eq 2, we have used a random-mixing approximation for the interaction energy. This approximation can also be used while placing the molecules in the system: the probability that a site on which a segment or molecule is to be placed is empty (the vacancy probability) is then equal to the volume fraction of empty sites. However, as we will be calculating the volume fraction per bond direction, it is possible to improve on the calculation of the vacancy probability as follows. Suppose we want to place a bond "up", *i.e.*, from layer z to layer $z + 1$. Then all segments in layer $z + 1$ which are part of a bond between z and $z + 1$ will not block this step. This means that the vacancy probability is greater than one would expect from a pure random mixing approximation, by a factor proportional to $1 - \varphi(z + 1|z)$. The last term is the volume fraction of segments having bonds between z and $z + 1$. Introducing $\varphi_i(z,s,d)$ as the volume fraction of segment s of molecule i in layer z with its bond to segment $s + 1$ in direction d, we can write for the weighting factor $g(z + d|z)$ for a bond between $z + d$ and z:

$$g(z+d|z) = \frac{1 - \sum_{\mathrm{i}} \varphi_{i,d}^{\mathrm{bulk}}}{1 - \sum_{\mathrm{i}} \varphi_i(z+d|\mathrm{z})} \tag{4}$$

where

$$\varphi_i(z+d|z) = \sum_s (\varphi_i(z,s,d) + \delta(|d|,1)\varphi_i(z+d,s,-d)) \tag{5}$$

is the volume fraction of bonds that molecule i has in layer z. The Kronecker δ factor $\delta(|d|,1)$ is inserted to ensure that bonds within layer z are not counted twice. The parameter $\varphi_{i,d}^{\mathrm{b}}$ is defined as

$$\varphi_{i,d}^{\mathrm{b}} = \varphi_i^{\mathrm{b}} \frac{N_i - 1}{3N_i} \tag{6}$$

and denotes the relative number of bonds of i in direction d in the bulk solution. The factor ${}^1/_3$ stems from the use of a cubic lattice: in general each direction contributes a factor $2/Z$, where Z is the coordination number of the lattice. The use of eqs 4−6 leads to an anisotropy in the polymer statistics. Therefore, it has been called SCAF, for self-consistent anisotropic field.[9] The self-consistency arises from the fact that the volume fractions of bonds are needed for the calculation of the weighting factors, but also the other way around: the weighting factors are needed for the calculation of the volume fractions of bonds. The SCAF can be seen as a first-order improvement on the random-mixing approximation, but it still implements a mean-field approach. The SCAF extension corrects the SCF theory for bond direction correlations through space, to be contrasted with the short-range bond orientation correlations along the chain which will be treated next.

Chain Stiffness in Polymer Statistics. In a cubic lattice, two consecutive bonds can have three relative orientations: a straight conformation, where a bond makes an angle of 180° with the preceding one, a perpendicular conformation of 90°, and direct backfolding, where the angle is 0°. We denote the energy difference between a straight conformation between the segments $s - 1$, s, and $s + 1$ and a perpendicular one as $\Delta U_{\mathrm{sp}}(s)$. Typically, $\Delta U_{\mathrm{sp}}(s)$ is negative. The weighting factor $\lambda_s(s)$ for a straight conformation is related to the weighting factor $\lambda_p(s)$ for a perpendicular conformation as

$$\lambda_s(s) = \lambda_p(s) \exp\left(-\frac{\Delta U_{\mathrm{sp}}(s)}{kT}\right) \tag{7}$$

for $1 < s < N$. We will exclude direct backfolding of two consecutive bonds, so that the weighting factor $\lambda_b(s)$ for backfolding is zero for $1 < s < N$. Everywhere along the chain, we must have

$$\lambda_b(s) + 4\lambda_p(s) + \lambda_s(s) = 1 \tag{8}$$

The end points only have one bond, so that $\lambda_b(s) = \lambda_p(s) = \lambda_s(s) = {}^1/_6$ for $s = 1$ and $s = N$.

Wijmans *et al.*[11] have shown that for a homopolymer (where ΔU_{sp} does not depend on the segment number) with infinite chain length there is a simple relation between the Kuhn length P, here defined as the number of bonds that are joined together in a Kuhn segment, and the bending energy ΔU_{sp}, namely

$$P = 1 + 0.5 \exp(-\Delta U_{\mathrm{sp}}) \tag{9}$$

Closely related to the Kuhn length is the persistence length, which is found by replacing the factor 0.5 in eq 9 by 0.25. Thus, when a polymer is not too flexible, there is just a factor of 2 between the Kuhn length and the persistence length. The statistical weight of a segment s of polymer i in layer z that will make a step in the direction d, given that the first segment is somewhere in the system, is called the end segment distribution function $G_i(z,s,d|1)$. As a starting condition we take

$$G_i(z,1,d|1) = G_i(z,1) \tag{10}$$

for any d. Here we have used a generalized free segment distribution function $G_i(z,1)$, which for an arbitrary segment number s is defined as $G_i(z,s) = G_A(z)$ if segment number s is of segment type A. Connecting the segments in a second-order Markov approximation yields

$$\begin{aligned} G_i(z,s,-1|1) = {} & \\ & G_i(z,s)\{\lambda_b(s)g(z-1|z)G_i(z-1,s-1,1|1) + \\ & 4\lambda_p(s)g(z|z)G_i(z,s-1,0|1) + \\ & \lambda_s(s)g(z+1|z)G_i(z+1,s-1,-1|1)\} \end{aligned} \tag{11a}$$

$$\begin{aligned} G_i(z,s,0|1) = {} & \\ & G_i(z,s)\{\lambda_p(s)g(z-1|z)G_i(z-1,s-1,1|1) + \\ & (2\lambda_p(s) + \lambda_s(s) + \lambda_b(s))g(z|z)G_i(z,s-1,0|1) + \\ & \lambda_p(s)g(z+1|z)G_i(z+1,s-1,-1|1)\} \end{aligned} \tag{11b}$$

$$\begin{aligned} G_i(z,s,1|1) = {} & \\ & G_i(z,s)\{\lambda_s(s)g(z-1|z)G_i(z-1,s-1,1|1) + \\ & 4\lambda_p(s)g(z|z)G_i(z,s-1,0|1) + \\ & \lambda_b(s)g(z+1|z)G_i(z+1,s-1,-1|1)\} \end{aligned} \tag{11c}$$

where $g(z+d|z)$ is defined in eq 4. Starting from the other side of the chain, we have to keep in mind that the bonds are defined from segment s to segment $s + 1$, and the conformations are now between the segments s, $s + 1$, and $s + 2$. This leads to an asymmetry in the end segment distribution functions: $G_i(z,s,d|N)$ is the statistical weight of segment s of polymer i to have reached layer z coming from the direction d, with the end segment N somewhere in the system. The starting condition is

$$G_i(z,N,d|N) = G_i(z,N) \tag{12}$$

as in (9). The other segments are connected using

$$\begin{aligned} G_i(z,s,-1|N) = {}& \\ G_i(z,s)g(z+1|z)\{&\lambda_b(s+1)G_i(z+1,s+1,1|N) + \\ &4\lambda_p(s+1)G_i(z+1,s+1,0|N) + \\ &\lambda_s(s+1)G_i(z+1,s+1,-1|N)\} \end{aligned} \tag{13a}$$

$$\begin{aligned} G_i(z,s,0|N) = {}& \\ G_i(z,s)g(z|z)\{&\lambda_p(s+1)G_i(z,s+1,1|N) + \\ &(2\lambda_p(s+1) + \lambda_s(s+1) + \lambda_b(s+1))G_i(z,s+1,0|N) + \\ &\lambda_p(s+1)G_i(z,s+1,-1|N)\} \end{aligned} \tag{13b}$$

$$\begin{aligned} G_i(z,s,1|N) = {}& \\ G_i(z,s)g(z-1|z)\{&\lambda_s(s+1)G_i(z-1,s+1,1|N) + \\ &4\lambda_p(s+1)G_i(z-1,s+1,0|N) + \\ &\lambda_b(s+1)G_i(z-1,s+1,-1|N)\} \end{aligned} \tag{13c}$$

Finally, two end segment distribution functions can be joined to find the segment density profile:

$$\varphi_i(z,s,d) = C_i\lambda_d\frac{G_i(z,s,d|N)G_i(z,s,-\mathrm{d}|1)}{G_i(z,s)} \tag{14}$$

where C_i is a normalization constant. For a polymer in full equilibrium, C_i is equal to φ_i^b/N_i. Equation 14 is called the composition law. It relates volume fractions via chain statistics to (potential) energies. However, the energies depend on the volume fractions (eq 2 and the space-filling constraint), so that, as with the bond correlations, we have a self-consistent set of equations that has to be solved numerically.

Results

General aspects of polymer adsorption have been discussed thoroughly in the literature.[12] In ref 13 it was shown that for the case of adsorption from a dilute solution the volume fraction profile consists of the three parts proposed by de Gennes:[14] a proximal regime, which for high adsorption energies consists of only one lattice layer; a central regime showing a power law decay $\varphi(z) \propto z^{\alpha}$, with α depending on chain length and bulk volume fraction; and a distal regime far from the surface, where the volume fraction decays exponentially as $\varphi(z) \propto \exp(-\gamma z)$, with γ inversely proportional to the radius of gyration. If the polymer adsorbs from a semidilute solution, the profile is independent of chain length,[15] again in agreement with the scaling analysis of de Gennes.[14] With the theory presented above, we can check whether these scaling results still apply for semiflexible polymers. Also, as the rigidity is defined to be a local parameter (*i.e.*, it depends on the segment ranking number), it is possible to model block copolymers with blocks having different rigidity. In doing such, we can distinguish between energetic and entropic driving forces for adsorption. Entropic factors are usually neglected, and it remains to be seen whether this is justified or not. Unless stated otherwise, we have taken $g(z+d|z)$ to equal 1, *i.e.*, we did not use the SCAF extensions.

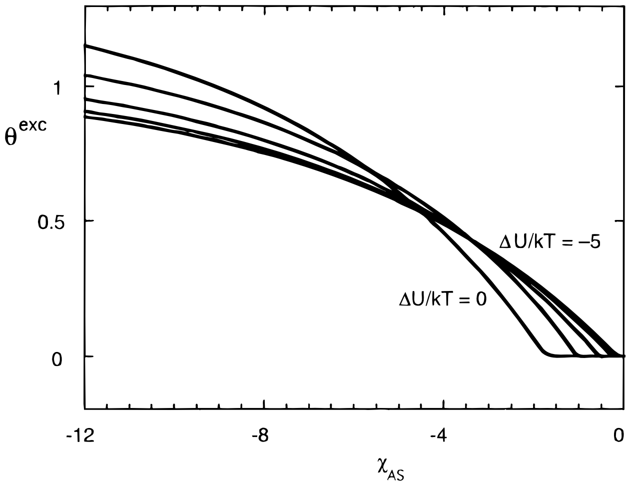

Figure 1. Excess amount of a homopolymer with 1000 segments adsorbed from an athermal monomeric solvent as a function of the adsorption energy χ_{AS}. The energy difference between a straight and a perpendicular bond ΔU_{sp} was varied as 0, −1, −2, −3, −4, and −5 kT. The polymer volume fraction in the bulk solution is 10^{-4}.

Critical Adsorption Energy. We consider the case of a homopolymer adsorbing from a monomeric solvent. Such a polymer is restricted in the number of conformations that it can assume near an impenetrable interface, and this entropy loss must be compensated for. If the adsorption energy is not sufficiently negative, the polymer molecules will avoid the interface. This leads to the concept of a critical adsorption energy which is, in contrast to the adsorption energy parameter χ_{AS}, independent of the kind of solvent used. In the limit of infinitely long freely jointed chains on a cubic lattice, the critical adsorption energy is $\chi_{AS}^{cr} = 6\ \ln(^5/_6)$, corresponding to $\chi_s^{cr} = \ln(^6/_5)$, independent of the segment type.

Birshtein *et al.*[16] derived that the critical adsorption energy in the limit of infinite chain length becomes a function of the Kuhn length P. Their result can be written as

$$\chi_{AS}^{cr} = 6\ \ln\left(\frac{P + \sqrt{P^2 + 4}}{2P + 2}\right) \tag{15}$$

which indicates that in the limit of rigid rods ($P \to \infty$) the critical adsorption energy approaches zero as there is no conformational entropy loss. Note that $P = 1$ in their model does not exactly give the freely jointed chain result, since direct backfolding is prohibited.

In order to investigate how the critical adsorption energy of polymer chains of finite chain length, adsorbing from a monomeric solvent, depends on the flexibility of the chain, we have conducted a number of calculations. The results are presented in Figure 1. In this figure the excess amount θ_i^{exc}, defined as $\theta_i^{exc} = \sum_z(\varphi_i(z) - \varphi_i^b)$, is plotted as a function of the adsorption energy for a homopolymer consisting of 1000 segments. We find a shift in the critical adsorption energy to less negative values. This is easily explained by the fact that stiff molecules lose less entropy per segment than fully flexible ones. In Figure 2a we have plotted the critical

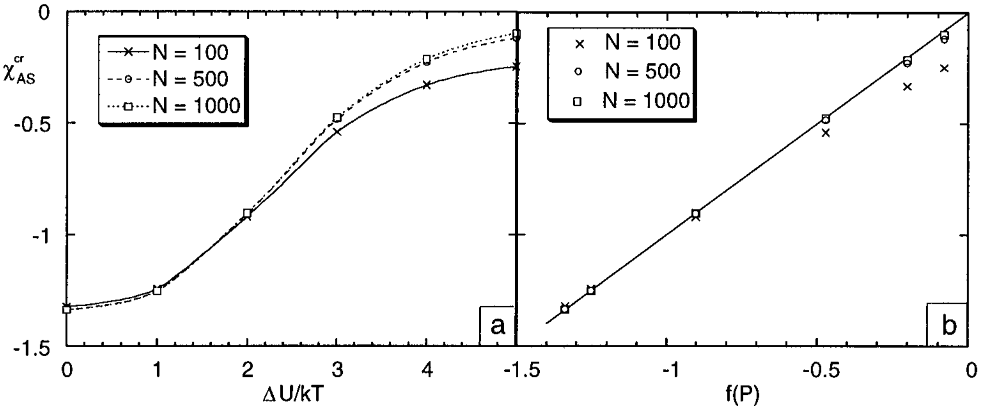

Figure 2. (a) Critical adsorption energy for three polymers of different chain length, which adsorb from an athermal monomeric solvent as a function of the energy difference $\Delta U = -\Delta U_{sp}$ between straight and perpendicular bond orientations. Athermal solvent, polymer bulk volume fraction $\varphi^b = 10^{-7}$. (b) Critical adsorption energy plotted as a function of $f(P)$, where P is the Kuhn length and $f(P) = 6 \ln[(P + (P^2 + 4)^{1/2}/(2P + 2)]$. The full line is the prediction by the analytical theory of Birshtein *et al.* (eq 15). Other parameters as in (a).

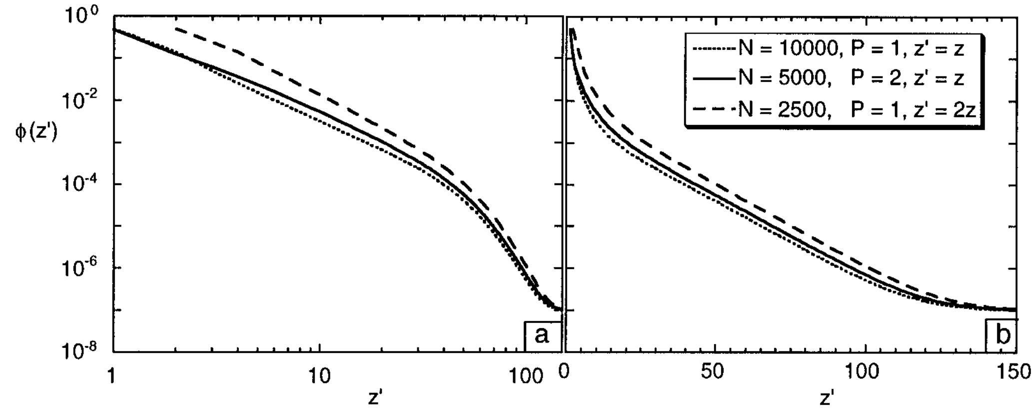

Figure 3. Volume fraction profiles for a homopolymer with (i) chain length 5000 using second-order Markov statistics, no backfolding ($\lambda_b = 0$), and $\Delta U_{sp}/kT = -\ln 2$; (ii) chain length 10 000 using first-order Markov statistics; and (iii) chain length 2500 using first-order statistics and plotted against $2z$ instead of z. Adsorption energy, $\chi_{AS} = -6$; other parameters as in Figure 2.

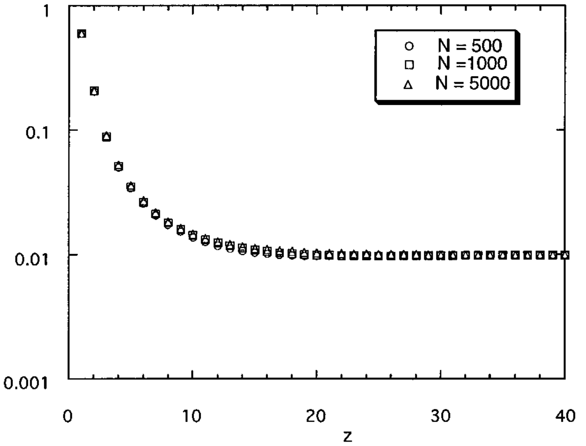

Figure 4. Volume fraction profiles in the semidilute regime ($\varphi^b = 0.01$) for homopolymers with 500, 1000, and 5000 segments using second-order Markov statistics, no backfolding ($\lambda_b = 0$), $\Delta U_{sp}/kT = 0$, and a SCAF approach.

adsorption energy as a function of the straight–perpendicular energy difference ΔU_{sp}. The critical adsorption point is defined by the surface affinity for which $\theta^{exc} = 0$. In this figure, we note that at high absolute values of ΔU_{sp} the critical adsorption energy becomes almost independent of ΔU_{sp}. In Figure 2b we check the prediction of eq 15. If the numerical results would be predicted perfectly by eq 15, then all points should fall on the solid line. We see that the agreement with the analytical theory is excellent. Naturally the long chains follow the predictions of eq 6 to a higher degree of stiffness than the shorter ones.

Rescaling and the Kuhn Length. As already stated, the radius of gyration of an ideal semiflexible polymer can be rescaled to a polymer with less segments, but with a longer Kuhn length. Fleer *et al.*[12] ventured that this procedure might also be used in the case of polymer adsorption. This idea was based upon results of Leermakers *et al.*;[8] however, their results are for a melt and might not apply to dilute solutions. In practice, the value taken for the ratio between the Kuhn length and the bond length is the so-called characteristic ratio, which is tabulated for a large variety of polymers.[17] In a lattice theory, the Kuhn length is usually taken to equal the lattice spacing for convenience. Thus, in the first-order Markov statistics used in the standard Scheutjens and Fleer scheme, we take the Kuhn length P to be 1, and for the second-order statistics we use eq 9. As an example, we take a homopolymer containing 5000 segments with $\Delta U_{sp}/kT = -\ln 2$, so that $P = 2$, according to eq 9. There are now two ways to rescale this polymer to a fully flexible one with $P = 1$: by halving the chain length, which should be accompanied by a doubling of the lattice spacing (case I), or by doubling the chain length without changing the lattice spacing (case II). The resulting volume fraction profiles are plotted in Figure 3: the dashed curve is case I, the dotted curve case II. In Figure 3b, where the profiles are plotted on a log–lin scale, we can check that the radius of gyration is indeed scaled back properly as the curves run parallel in the distal regime: the exponent in the distal regime scales with the inverse of the correlation length in the dilute solution,[13,14] which equals the inverse radius of gyration. However, the log–log scale in Figure 3a shows clearly that the behavior in the central regime differs considerably in both cases. The difference could be due to the fact that resizing the polymer or the lattice spacing changes the conformational entropy of the polymer, and it is not obvious whether or not the difference in entropy is the same in the bulk as near the surface. A recent theory by Ploehn[18] allowing for a difference in molecular volume between polymer and solvent seems to indicate that indeed there is a problem here.

We conclude that rescaling does not work in the case of polymer adsorption, which indicates that for adsorption the characteristic ratio is a relevant parameter. The rescaling failed because the characteristic ratio is not conserved in the rescaling procedure. Another conclusion that can be drawn from this example is that one cannot expect experimental volume fraction profiles to coincide with calculated ones if the characteristic ratio is used to rescale the molecular weight of the polymer to the number of segments per chain used in the model.

Influence of Bond Correlations. It has been shown[15] that the volume fraction profile in the case of a polymer adsorbing from an athermal semidilute solution is independent of the chain length. This universality should also be independent of the details of the model used, as it derives from the general idea that in a semidilute solution the chain length is not a predominant parameter. With the use of the SCAF, equations for thermodynamic parameters like the partition function, (excess) free energy, and chemical potential differ significantly from the ones without the SCAF, even though both approaches use a mean-field approximation.[9] The SCAF was originally used for chains in a rotational isomeric state (RIS) scheme. RIS applies third-order Markov statistics and was devised by Volkenstein[19] to incorporate trans–gauche isomerism in polymer statistics. The cubic lattice scheme is computationally much faster than RIS, enabling the modeling of longer molecules.

Figure 4 shows the volume fraction profile for polymers with different chain lengths. It can be seen that again the profile is hardly dependent on chain length. It must be noted that these profiles do not coincide with the profiles using only first-order statistics or even only second-order Markov statistics: each model has its own profile, independent of the chain length. Of course, other theoretical models, not using a mean-field approximation, should be applied to test the chain-length independence of the profile. Unfortunately, models like Monte Carlo or molecular dynamics are not easily used for the long chains needed to find this universal behavior.

Stiff–Flexible Copolymers. In writing down the chain statistics, care was taken to have the bending energies depend on the segment ranking number. This enables us to model a copolymer where the constituent monomers differ in stiffness. In practice, this is often the case: *e.g.*, for polystyrene, the characteristic ratio is 2.6 times as large as for poly(ethylene oxide). This difference in rigidity creates an entropic reason for the stiffer parts to adsorb preferentially over the flexible ones. In order to distinguish the entropic factors from the energetic factors, all Flory–Huggins parameters will be taken equal for all blocks. For a straight or perpendicular local conformation, two bonds are needed. If we have a block copolymer with two segment types A and B, then there are four sequences of segments playing a role: AAA, AAB, ABB, and BBB, which all have a different energy. To simplify the calculations, we have taken ΔU_{sp} to depend only on the segment type of the middle segment. Thus, for AAA and AAB we take the energy difference belonging to the A blocks, and for ABB and BBB that of the B blocks. This is only a minor simplification for block copolymers, since it affects only the segments next to the joint between two blocks. As an example, we take two polymers with 1001 segments. The first one is denoted A_{1001}, and is a semiflexible homopolymer: $\Delta U_{\mathrm{sp}}/kT = -1$ for all segments. The second one, $A_{100}B_{800}A_{101}$, is a copolymer with 200 stiff

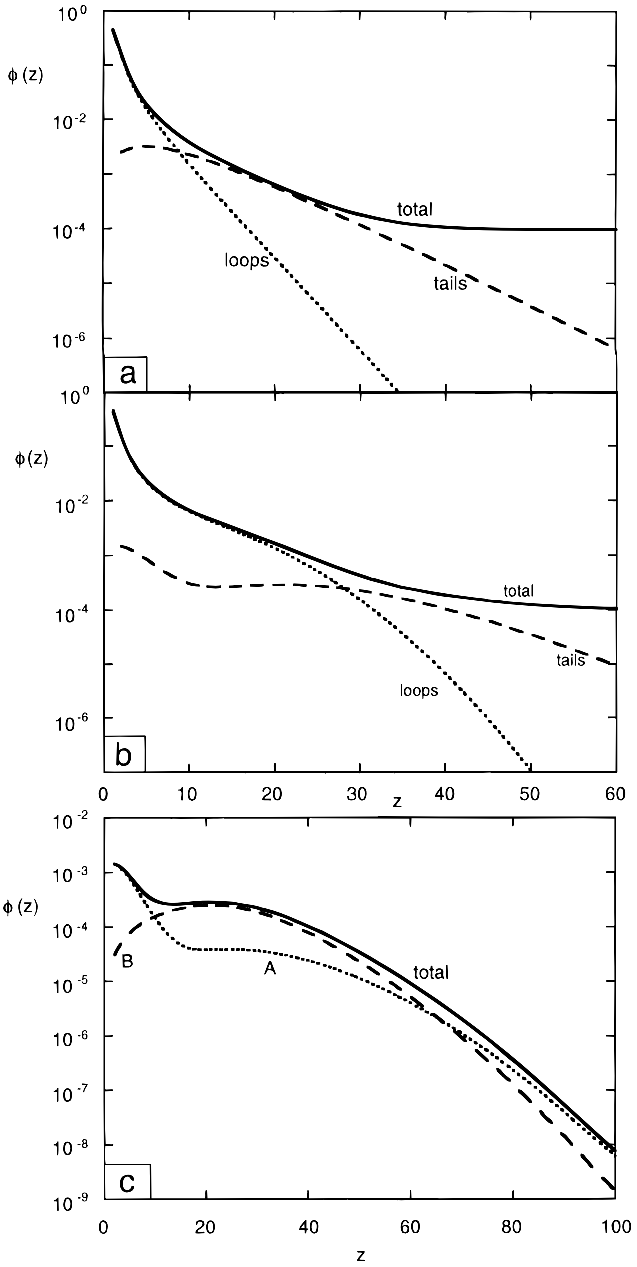

Figure 5. Volume fraction profiles for a polymer with 1001 segments, using second-order Markov statistics. In diagram a, all segments have the same bending energy difference, $\Delta U_{\mathrm{sp}}(s)/kT = -1$; in (b) segments 1–100 and segments 900–1001 have $\Delta U_{\mathrm{sp}}(s)/kT = -1$; the other segments are flexible with $\Delta U_{\mathrm{sp}}(s)/kT = 0$. Bulk volume fraction, $\varphi^{\mathrm{b}} = 10^{-4}$; adsorption energy, $\chi_{\mathrm{AS}} = -6$; athermal solvent. Diagram c gives the tail profile from (b) and the contributions to it due to both segment types.

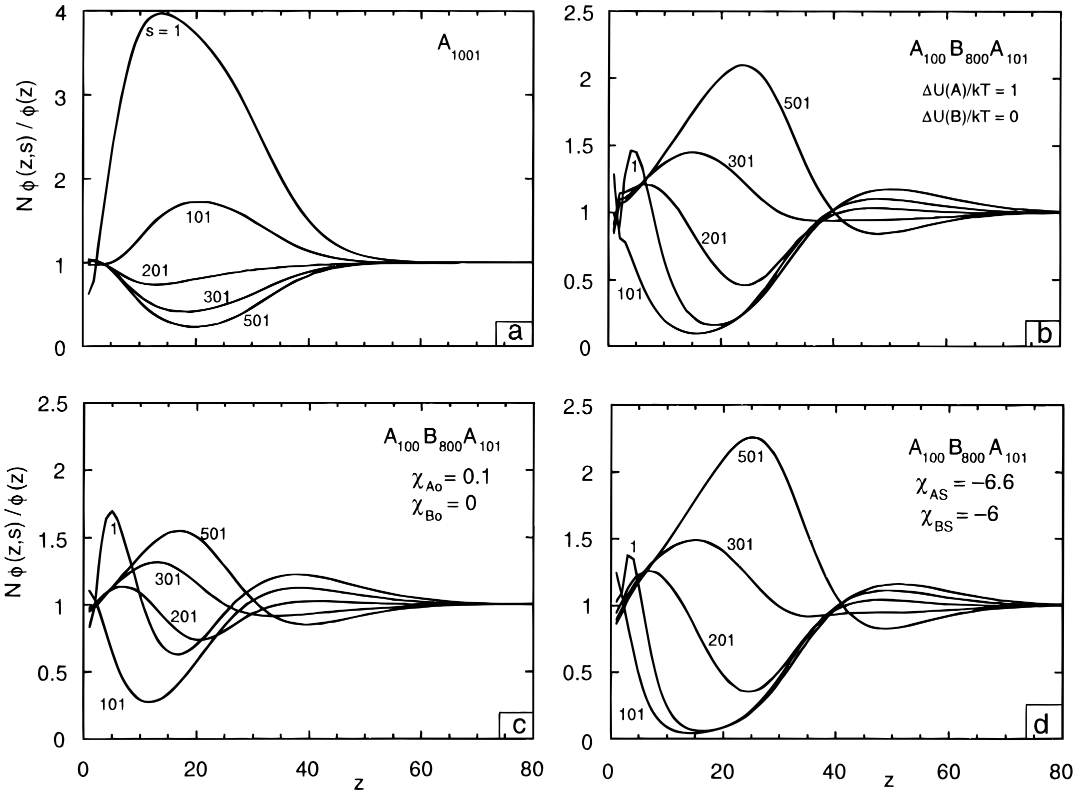

Figure 6. Relative preference profiles for several segments of different polymers. Diagrams a and b as in Figure 5; diagrams c and d refer to flexible copolymers $A_{100}B_{800}A_{100}$ with $\Delta U_{sp}(s)/kT = 0$ for all s. In diagram c there is a difference in solvency: $\chi_{Ao} = 0.1$, $\chi_{Bo} = 0$, and $\chi_{AS} = \chi_{BS} = -6$. In diagram d there is a difference in adsorption energy: $\chi_{AS} = -6$, $\chi_{BS} = -6$, and $\chi_{Ao} = \chi_{Bo} = 0$. Segment numbers are indicated.

($\Delta U_{sp}/kT = -1$) bonds, 100 on each end, whereas the middle 800 bonds are flexible: $\Delta U_{sp}/kT = 0$. Figure 5 shows the volume fraction profiles, with diagram a for the homopolymer and diagram b for the copolymer. The volume fractions of the loops and tails of the polymers were calculated using the method outlined in ref 20. It turns out that the stiffness disparity in the copolymer leads to long loops, protruding far into the solution. This gives a hydrodynamic layer thickness[21] 1.9 times as large as the homopolymer case, whereas the excess amount is only 1.07 times as large. The tail profile shows two maxima. This can be explained using Figure 5c, where the tail profile is split up into the contributions due to the different segment types. It can be seen that the first maximum is due to the end (A) segments and the second maximum to the middle (B) segments. Furthermore, the periphery of the profile consists again of A segments. This suggests that the polymer behaves like a telechelic polymer as modeled by Wijmans *et al.*[22] In analogy to their results, we can expect bridge formation and thus flocculation if two surfaces covered with these polymers are brought together.

The idea of telechelic behavior is further corroborated by Figure 6, where we plot the relative preference of a segment to be in layer z, defined as $N\varphi(z,s)/\varphi(z)$, for five different segments distributed over the molecule: s = 1 corresponds to an end segment, for the copolymer s = 101 is at the joint of two blocks, and s = 201, 301, and 501 relate to various positions in the central B block. Diagram a shows the typical homopolymer segment distribution as already shown in ref 21: the ends are on average further from the surface, because the tails protrude far into the solution. On the other hand, the middle segments prefer to be close to the surface. For the block copolymer in (b), this picture changes drastically: the first segment shows two maxima in the preference profile: one in the second layer, corresponding to tail adsorption, and one around layer 50, indicating a stretched conformation. The middle segments are now sticking out into the solution, showing again that large loops are formed. Thus, we have managed to create a system where the polymer tails adsorb preferentially for purely entropic reasons.

For comparison, preference plots are also shown for a fully flexible copolymer, where the solvent is slightly worse for the A blocks ($\chi_{Ao} = 0.1$ and $\chi_{Bo} = 0$, Figure 6c), and for a flexible copolymer, where the A segments have slightly more adsorption energy than the B segments ($\chi_{AS} = -6.6$ and $\chi_{BS} = -6$, Figure 6d). The shape of these plots is the same as Figure 6b, again indicating that a difference in rigidity has the same effect as a difference in interaction energy. Also, the effects are of the same order of magnitude. We may conclude that it is not justified to neglect rigidity differences between the blocks of a copolymer.

As a last example for stiff−flexible copolymers, we show in Figure 7 the effect of the relative location of the stiff block. Again, we have 200 stiff bonds, with $\Delta U_{sp}/kT = -1$, and 800 flexible ones, with $\Delta U_{sp}/kT = 0$. The full curve refers to the case where all the stiff segments are joined in one block and moved along the molecule. It turns out that the excess amount (Figure 7a) does not vary much, but the hydrodynamic layer thickness (Figure 7b) does so considerably. If the adsorbing block is located at the end (x = 0) the adsorbed polymer layer can be regarded as a brush: one tail is sticking out into solution. If the adsorbing block is located in the middle (x = 400), there are two tails, which are necessarily shorter. This leads to the interesting effect that the hydrodynamic layer thickness decreases where the excess amount (which for these low bulk volume fractions equals the adsorbed amount)

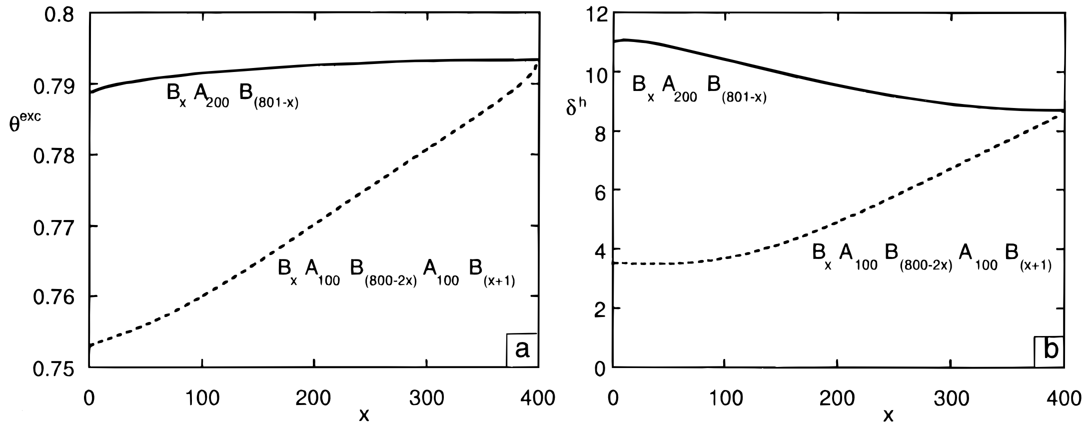

Figure 7. (a) Excess amount and (b) hydrodynamic layer thickness of block copolymers having 200 rigid bonds, associated with the A segments, and 800 flexible bonds at the B segments. Full curve, asymmetric copolymers $B_xA_{200}B_{(801-x)}$; dashed curve, symmetric copolymers $B_xA_{100}B_{(800-2x)}A_{100}B_{(x+1)}$. For $x = 400$, both cases correspond to the same molecule. Bulk volume fraction, $\varphi^b = 10^{-7}$; other parameters as in Figure 5b.

increases. The dashed curve shows the symmetrical case, in which the stiff segments are split into two blocks of 100 stiff bonds each. For small x we have the situation of Figure 6b: the polymer is forced to make long loops and hardly any tails are present. This leads to a small hydrodynamic layer thickness, more than 3 times lower than in the symmetrical case, whereas the difference in excess amount is only about 5%. Upon increasing x, tails are being formed. As this is entropically favorable, the adsorption goes up slightly. But initially this does not increase the layer thickness, as the tails grow at the cost of the loops dominating in the outer layers. Only when the tails are sufficiently large can the hydrodynamic layer thickness go up.

Conclusions

Second-order Markov statistics in a cubic lattice are computationally the simplest way to model chain stiffness. It is possible to model copolymers where parts of the molecule are stiffer than other parts (stiff–flexible copolymers). Using this concept, it is shown that end blocks can adsorb preferentially on the surface for purely entropic reasons if their stiffness is larger than that of the middle block. This effect is of the same order of magnitude as energetic interactions, so that neglecting rigidity differences between blocks seems unjustified. For homopolymers, our model reproduces the predictions of Birshtein *et al.* regarding the dependence of the critical adsorption energy on the rigidity. Although the radius of gyration for a stiff polymer in a dilute solution can be rescaled to a flexible polymer by increasing the step length, this procedure does not work for the adsorption profile of a polymer adsorbing from a dilute solution. The fundamental reason for this is that the characteristic ratio is not conserved in rescaling attempts. The characteristic ratio is apparently important in a lattice-based description of polymer adsorption (and may be so for real systems). In the case of adsorption from a semidilute solution, we have shown that incorporating bond correlations does not alter the chain-length independence of the volume fraction profile.

References and Notes

(1) Kuhn, W. *Kolloid Z.* **1934**, *68*, 2.
(2) Kratky, O.; Porod, G. *Recl. Trav. Chim. Pays-Bas* **1949**, *68*, 1106–1122.
(3) Maggs, A. C.; Huse, D. A.; Leibler, S. *Europhys. Lett.* **1989**, *8*, 615–620.
(4) Odijk, T. *Macromolecules* **1986**, *19*, 2313–2329.
(5) Yethiraj, A.; Kumar, S.; Hariharan, A.; Schweizer, K. S. *J. Chem. Phys.* **1994**, *100*, 4691–4694.
(6) Scheutjens, J. M. H. M.; Fleer, G. J. *J. Phys. Chem.* **1979**, *83*, 1619–1635.
(7) Evers, O. A.; Scheutjens, J. M. H. M.; Fleer, G. J. *Macromolecules* **1990**, *23*, 5221–5233.
(8) Leermakers, F. A. M.; Scheutjens, J. M. H. M.; Gaylord, R. J. *Polymer* **1984**, *25*, 1577–1588.
(9) Leermakers, F. A. M.; Scheutjens, J. M. H. M. *J. Chem. Phys.* **1988**, *89*, 6912–6924.
(10) Silberberg, A. *J. Chem. Phys.* **1968**, *48*, 2835–2851.
(11) Wijmans, C. M.; Leermakers, F. A. M.; Fleer, G. J. *J. Chem. Phys.* **1994**, *101*, 8214–8223.
(12) Fleer, G. J.; Cohen Stuart, M. A.; Scheutjens, J. M. H. M.; Cosgrove, T.; Vincent, B. *Polymers at interfaces*; Chapman & Hall: London, 1993.
(13) van der Linden, C. C.; Leermakers, F. A. M. *Macromolecules* **1992**, *25*, 3449–3453.
(14) de Gennes, P.-G. *Macromolecules* **1981**, *14*, 1637–1644.
(15) van der Linden, C. C. Polymer adsorption theory; universal aspects and intricacies. Ph.D. Thesis, Wageningen Agricultural University, Wageningen, The Netherlands, 1995.
(16) Birshtein, T. M.; Zhulina, E. B.; Skvortsov, A. M. *Biopolymers* **1979**, *18*, 1171–1186.
(17) Brandrup, J.; Immergut, E. H. *Polymer Handbook*; J. Wiley & Sons: New York, 1989.
(18) Ploehn, H. J. *Macromolecules* **1994**, *27*, 1617–1626.
(19) Volkenstein, M. V. *Configurational statistics of polymeric chains*; John Wiley & Sons, Ltd.: London, 1963; Vol. XVII.
(20) Scheutjens, J. M. H. M.; Fleer, G. J. *J. Phys. Chem.* **1980**, *84*, 178–190.
(21) Scheutjens, J. M. H. M.; Fleer, G. J.; Cohen Stuart, M. A. *Colloids Surf.* **1986**, *21*, 285–306.
(22) Wijmans, C. M.; Leermakers, F. A. M.; Fleer, G. J. *J. Colloid Interface Sci.* **1994**, *167*, 124–134.

MA950400K